SPH simulations of buoyant and non-buoyant jets into open-channel flows

I. Federico[1], S. Marrone[2,3], F. Aristodemo[1], A. Colagrossi[2], P. Veltri[1]
[1]Dipartimento di Difesa del Suolo, Università della Calabria, Italy (federico@dds.unical.it)
[2] CNR-INSEAN, The Italian Ship Model Basin, Italy
[3] Dipartimento di Meccanica e Aeronautica, Università di Roma "Sapienza", Italy

***Abstract*—Flow phenomena induced by jet intake in a water body occur in natural environments such as pollutant discharge in rivers and engineering applications such as marine waster water outfalls. A study of buoyant and non-buoyant jets propagating into open-channel flows has been performed through a 2D SPH modelling.**

Two-phase flows in open channels are treated through an appropriate algorithm to model inlet/outlet boundary conditions. SPH equations of fluid mechanics are coupled with a SPH form of advective diffusion equation to treat different ranges of pollutant-water density ratios. Attention is paid to determine the induced flow and concentration field due to the interaction between the jet and the ambient flow.

SPH simulations of coflow and crossflow jets in buoyant and non-buoyant conditions have been carried. The model has been validated near the jet nozzle and far from it, comparing the numerical jet trajectories, velocities and concentration fields with the analytical ones.

I. Introduction

Jets have been investigated intensively for many years by the fluid mechanics community (see *e.g.* [1], [2]). The interest comes from the importance of these phenomena in several environmental and industrial flows. Jet discharges from industrial and domestic sources often enter rivers and marine areas. This flow configuration is of theoretical significance in environmental hydraulics and fluid mechanics due to the complex interaction between a jet and an ambient flow. This interaction leads to large-scale vortical structures which play a fundamental role in the entrainment of the ambient fluid into the discharge jet. In addition the transport process gives rise to mixing and dilution processes of the jet [3]. The present analyses are addressed to investigate buoyant and non-buoyant jets in shallow water streams.

SPH modelling of continuous jet discharges in open-channel flows needs appropriate inlet/outlet boundary conditions. As is common knowledge, the enforcement of these conditions is not trivial for Lagrangian particle models. Some researches have developed SPH models to treat upstream/downstream conditions in order to simulate uniform flows [4], [5]. Federico et al. [6] have proposed a suitable SPH-based algorithm to model these boundary conditions in handling different flow regimes in water streams. In this work, initial velocities, pressures and water depths both upstream and downstream in the computational domain are defined. Here, the basis of the computational method given by Federico et al. [6] is extended to model continuous two-phase fluids through the intake of tracer with the same or a different density as the surrounding open-channel flow. In order to determine the main flow phenomena induced by jet-water interaction, appropriate inflow-jet particles are introduced at different locations to simulate crossflow and coflow jets. SPH equations of fluid mechanics [7] are coupled with an advective diffusion SPH model [8] to simulate the flow field and the consequent mass transport for different range of jet-water density ratios. SPH simulations are performed in near field and far one.

In the following section the adopted SPH governing equations are recalled. Afterwards the algorithm to model jets in a finite open-channel flow through appropriate boundary conditions is illustrated. Comparisons of the proposed SPH model with analytical solutions are reported, showing the evolution of jet trajectories, velocities and concentrations given by the two-phase fluid interaction.

II. Numerical scheme

A. Governing equations

The reference equations for the flow evolution assuming a weakly-compressible fluid are:

$$\begin{cases} \dfrac{D\mathbf{v}}{Dt} = -\nabla p + \rho\,\mathbf{f} + \nabla\cdot\mathbf{V} + \mathbf{F}_s \\ \dfrac{D\rho}{Dt} = -\rho\nabla\cdot\mathbf{v} \\ p = c_0^2\,(\rho-\rho_0) \end{cases} \tag{1}$$

where $\mathbf{v}$, p and ρ are, respectively, the velocity, pressure and density of a generic material point, $\mathbf{f}$ represents the mass force acting on the fluid, ρ_0 the initial density at the free surface, c_0 the initial sound speed, $\mathbf{V}$ the viscous stress tensor and $\mathbf{F}_s$ the surface tension forces. The continuum equations proposed by Grenier et al [7] are here used to model two-phase flows. The SPH scheme is:

$$\begin{cases} \dfrac{D\mathbf{u}_a}{Dt} = -\dfrac{1}{\rho_a}\displaystyle\sum_b \left(\frac{p_a}{\Gamma_a}+\frac{p_b}{\Gamma_b}\right)\nabla_a W(\mathbf{r}_{ab})\,\Delta V_b + \\ \\ +\chi\displaystyle\sum_{b\in X^\zeta}\left(\left|\frac{p_a}{\Gamma_a}\right|+\left|\frac{p_b}{\Gamma_b}\right|\right)\nabla_a W(\mathbf{r}_{ab})\,\Delta V_b \\ \\ \rho_a = \displaystyle\sum_{b\in X} m_b \frac{W(\mathbf{r}_{ab})}{\sum_{k\in X} W(\mathbf{r}_{ak})\Delta V_k} \\ \\ p_a = c_0^2\,(\rho_a-\rho_0) \end{cases} \tag{2}$$

The subscrips indicate the quantities associated with the a-th and b-th particles. The subscript k refers only to the particles belonging to the fluid X containing the particle a. In particular, being $\mathbf{r_a}$ the position of a a-th particle, $\mathbf{r}_{ab} = \mathbf{r}_a - \mathbf{r}_b$ and $\mathbf{r}_{ak} = \mathbf{r}_a - \mathbf{r}_k$. The symbol ΔV_b is the b-th particle volume and $V_b = m_b/\rho_b$ where m_b is the b-th particle mass (constant during the flow evolution). The symbol $W(\mathbf{r}_{ab})$ represents the kernel centered at the b-th particle position and evaluated at the a-th particle position and a denotes the gradient taken with respect to the coordinates of particle a. In the system (2) the value of ρ is calculated through a Shepard kernel [9]. The parameter χ ranges between 0.01 and 0.1, and the second summation of the first equation in system (2) is applied to all the particles which do not belong to the fluid of the a-th particle; the latter set of particles is noted by X^ζ.

In order to deeply investigate the physical processes due to the two-phase flow interaction, the evaluation of the flow and concentration field is required. Therefore the equations (1) are coupled with the classical advective diffusion equation [1]:

$$\frac{DC}{Dt} = D\,\nabla^2 C - \nabla\cdot(\mathbf{v}C) \tag{3}$$

where D is the diffusion coefficient and C is the concentration.

A host of processes in rivers lead to a mixing to occur much faster than by molecular diffusion alone [10]. Recently a SPH model is formulated to solve the advective diffusion equation [8], taking into account for the diffusion and advective contributions occurring when a tracer propagates into a water stream. Following the approach used by Cleary and Monaghan [11] for determining a SPH formalism of heat conduction equation, the rate of change of concentration, DC_a/Dt, for two-phase flows has been derived as follows:

$$\frac{DC_a}{Dt} = \sum_b \frac{m_b}{\rho_a\rho_b}\frac{4D_aD_b}{D_a+D_b}(\rho_a+\rho_b)\frac{\mathbf{r}_{ab}\cdot\nabla_a W(\mathbf{r}_{ab})}{\mathbf{r}_{ab}^2}C_{ab}$$

$$-\sum_b m_b\frac{C_b}{\rho_a}\,(\mathbf{v}_a-\mathbf{v}_b)\cdot\nabla_a W(\mathbf{r}_{ab}) \tag{4}$$

The proposed form (4) gives a smoothed density gradient at the contact surface of two fluids, preventing anomalous high values of the concentration and leading to a natural decay in the mixing processes [8].

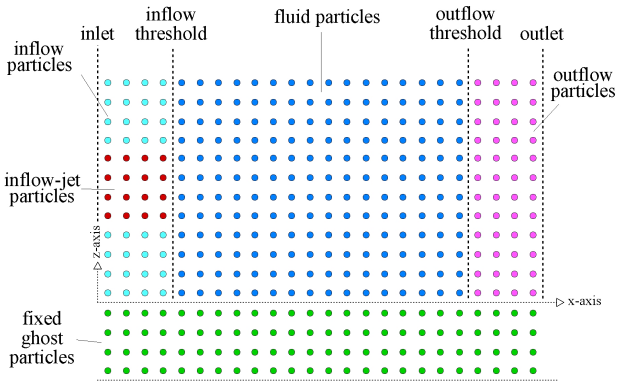

Fig. 1. Sketch of the computational domain: different colours are associated to different sets of particles.

B. Boundary conditions

Here, the techniques to model solid boundaries and enforce upstream and downstream boundary conditions are described.

The upstream and downstream boundary conditions are enforced through the in/out-flow algorithm proposed by Federico et al. [6]). In order to assign upstream and downstream flow conditions and model the jet injection, five sets of particles are defined as follows: fluid, fixed ghost, inflow, outflow and inflow-jet particles. Fig. 1 shows the initial sketch of the computational domain: different colours are associated to different sets of particles. In this case the jet input is located upstream the channel as an example of coflow jet. Further jet configurations are also adopted in the present paper to simulate crossflow jets. With reference to the computational procedure, the flow is directed along the x-axis and is limited by an inlet and an outlet boundary. An inflow and an outflow threshold are defined, the particles that cross these thresholds change the set they belongs to. The use of in/out-flow particles permits the imposition of different velocity both upstream and downstream in the computational domain. For what concern the water levels, only the upstream condition is assigned while the downstream one is determined by the flow evolution.

The solid boundaries are modeled through the fixed ghost particles approach (see [12]). In this technique, the ghost particles are fixed in the frame of reference of the body and are created only once at the beginning of the simulation. To compute the quantities attributed to each ghost particle, an interpolation point is associated to it. This interpolation point is obtained by mirroring the position of the fixed ghost particle into the fluid domain. Then, at each time step the physical quantities of the interpolation point are evaluated through a Moving Least-Square interpolation (see *e.g.* [13]) of the fluid particle values. In this way it is possible to enforce both Dirichlet and Neumann conditions.

III. Numerical simulations

A jet intake can be in the same direction as the ambient motion, in the opposite direction, perpendicular to the ambient motion, or at some intermediate angle. Here, attention is paid to the flows referred to non-buoyant coflow and crossflow jets, and buoyant crossflow jets.

For non-buoyant (advected) jets the initial momentum flux generally dominates the behaviour close to the nozzle. This type of flow is called strong jet and is weakly advected. The behaviour of the flow is similar to that of the simple jet. Further away from the source the entrained ambient momentum flux dominates the flow and the kind of flow changes. The flow is now said to be strongly advected. With reference to buoyant crossflow jets, the flow has initially a jet-like behaviour (strong jet). In this region, both the buoyancy-generated momentum flux and the entrained ambient momentum flux increase in size. If the buoyancy-generated momentum flux dominates after the strong jet region, the flow behaves like a plume. However, if the entrained ambient momentum flux dominates the flow after the strong jet region, the flow is an advected line momentum puff [14]. Fig. 2 shows a general sketch of the three simulated test cases, where the densities ρ_0 and ρ_1 refer to water and jet, respectively. The symbol U_0 refers to the initial horizontal velocity in the open channel, U_1 and V_1 to the horizontal and vertical velocity of the jet, and $U_e = U_1 - U_0$ to the excess velocity between the jet and the water.

A. Non-buoyant jets in crossflow

The first test case refers to a time-constant intake of tracer transversely to the open-channel flow direction. The open channel is characterized by $L = 20\,d$, where L is the water stream length and d is the jet diameter, $H = 20\,d$, being H the channel depth, and an initial horizontal velocity U_0 along x-axis. The jet with a velocity of V_1 along z-axis is injected perpendicularly to the incoming flow. Numerical simulations are carried out adopting the same density values between water (ρ_0) and jet (ρ_1). SPH results are compared with an analytical method for predicting the axis of core jets in cross-flow [15]:

$$x = \frac{C_d}{\pi}\frac{U_0^2}{V_1^2}\left(\frac{z}{d}\right)^2\left(1+\frac{Nz}{3d}\right)\,d \qquad (5)$$

where the coefficients were set equals to: $C_d = 1.5$ and $N = 5.2\,(V_1/U_0)^{-0.58}$.

Fig. 3 reports the comparisons between SPH simulations and analytical method proposed by Crowe and Riesebieter [15] in terms of axis of jet core, showing a general agreement between the solutions. The results are obtained for two initial velocity ratio between the vertical component of velocity of the jet and the horizontal component of velocity of the water body for $V_1/U_0 = 2.0$ (Fig. 3a) and $V_1/U_0 = 4.0$ (Fig. 3b).

The jet evolution into an uniform current using the proposed SPH model is highlighted, respectively, in Figs. 4a and 4c for the mentioned two velocity ratios. The jet trajectory is characterized by a progressive strong deflection of the axis core, particularly noticeable for $V_1/U_0 = 2.0$, due to its interaction with the incoming ambient flow. The increasing in velocity ratio leads to a growth of a relevant vortical structure in the clockwise direction [2]. Figs. 4b and 4d show the SPH simulations of the velocity field induced by jet-water interaction, in which the velocity $|v| = \sqrt{(u^2+v^2)}$ is reported. It can be observed a dispersion effect of the initial high values of V_1 into the ambient flow. The simulations are carried out for $t(U_0/d) = 10.0$, which represents a time duration long enough to reach steady state conditions. The adopted spatial resolution is $dx = 0.01d$.

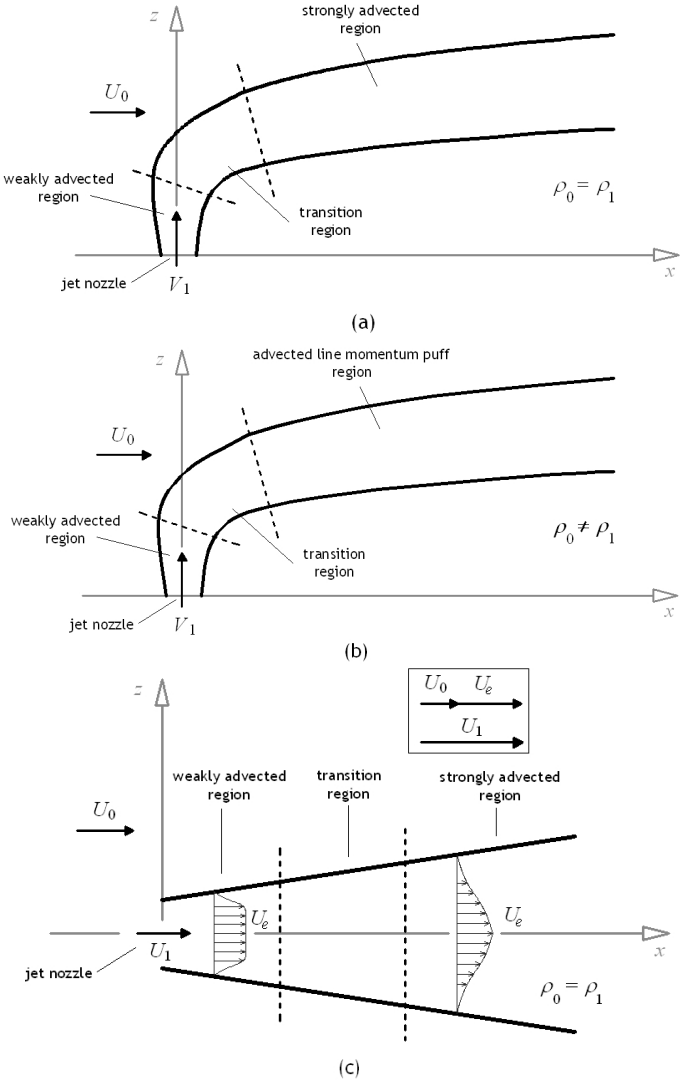

Fig. 2. Sketch of non-buoyant jet in crossflow (a), buoyant jet in crossflow (b) and non-buoyant jet in coflow (c).

B. Buoyant jets in crossflow

The second SPH simulation deals with a continuous buoyant jet in a crossflow condition. In particular, a buoyant jet is due to different densities between the jet and the surrounding flow ($\rho_0 \neq \rho_1$). They are common both in natural geophysical situations, but also in hydraulic, environmental and industrial

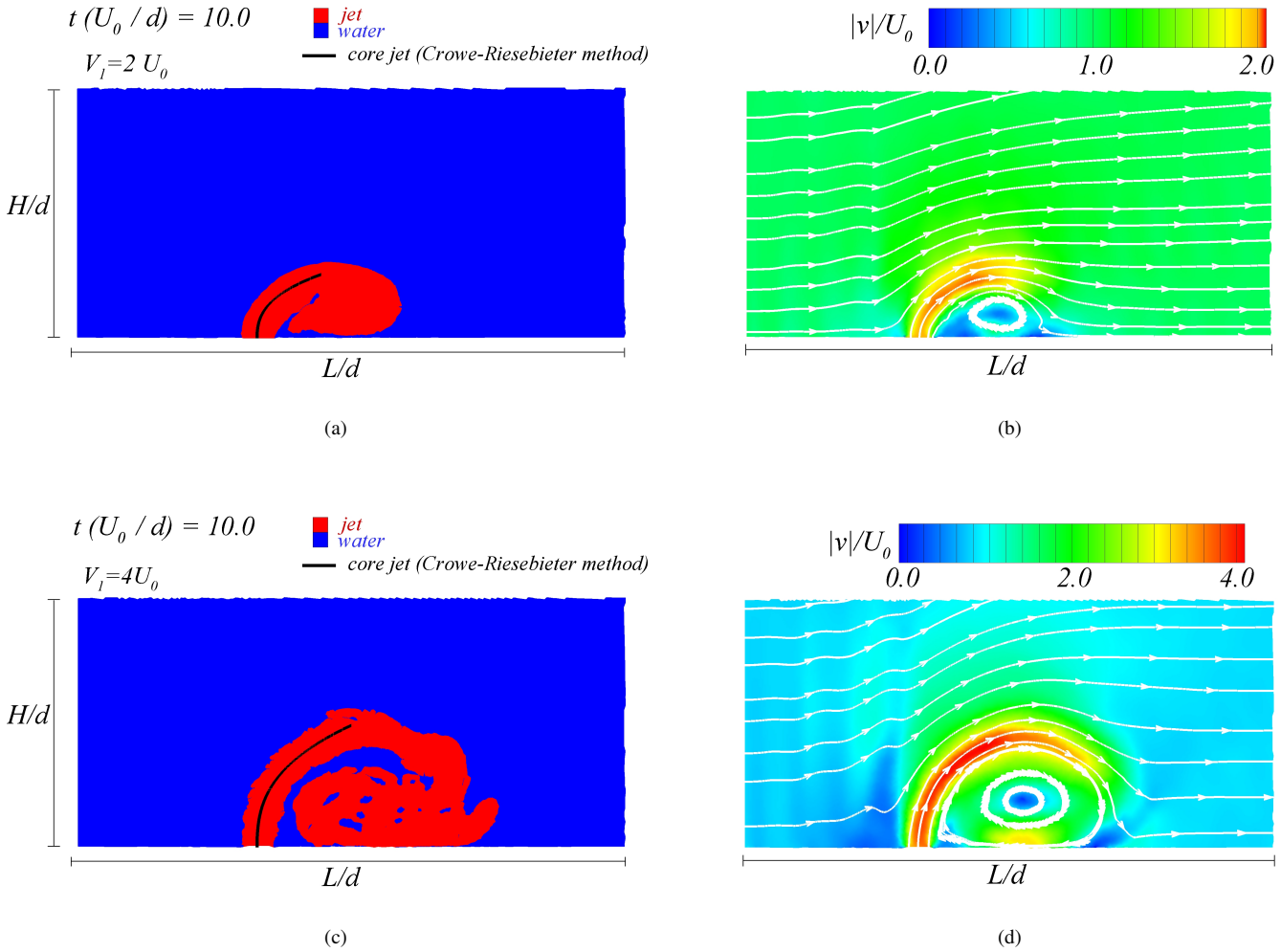

Fig. 3. SPH configuration of non-buoyant jets in crossflow at $t(U_0/d) = 10.0$ and comparison with analytical method for $V_1 = 2\,U_0$ (a) and $V_1 = 4\,U_0$ (c). SPH streamline velocity field [(b) and (f)].

applications, including various types of discharges into water streams or oceans in treatment facilities. The buoyancy of these discharges is usually due to differences in temperature, salinity or suspended solids [16].

The numerical water stream is defined through the following dimensions: $L = 20\,d$ and $H = 10\,d$. The velocity ratio is set equal to $V_1/U_0 = 2.0$ and the jet density, $\rho_0 = 1.030\rho_1$. This last ratio is typical for discharge of waste water in salt water as in the case of marine outfalls. The densimetric Froude number $Fr_1 = U_1/\sqrt{g'\,d}$ is set to 18, being $g' = g[(\rho_0 - \rho_1)/\rho_0]$ with g gravity acceleration.

The performances of the SPH model are validated against the following analytical relationship proposed by Papanicolaou et al. [17]:

$$z = \frac{l_M}{(RiR)^{-1/3}} \left(\frac{3}{\pi\sqrt{0.5}}\right) \left[RiR\frac{x}{l_M} + 0.5\left(RiR\frac{x}{l_M}\right)^2\right]^{1/3} \quad (6)$$

where $Q = V_1\,d$ is the specific mass flux, $M = Q\,V_1$ is the specific momentum flux, $B = [(\rho_0 - \rho_1)/\rho_0]\,g\,Q$ is the specific buoyancy flux. Being $l_M = M^{3/4}/B^{1/2}$ and $l_Q = Q/M^{1/2}$, the jet Richardson number is defined as $Ri = l_Q\,/\,l_M$.

Fig. 4 highlights the comparisons between SPH simulations and analytical method proposed by Papanicolaou [17] in terms of axis of jet centre, showing a general agreement between the solutions. The results refer to the weakly advected and transition regions. Also in this case, the simulations are carried out for $t(U_0/d) = 10.0$. The adopted spatial resolution is $dx = 0.075d$.

C. Non-buoyant jets in coflow

The last test case is referred to a continuous jet injected in a co-flowing environments. This kind of jet occurs when its direction is the same with respect to the surrounding flow. The simulations refer to a jet with $U_1 = 4\,U_0$ in a open-channel flow characterized by $L = 20\,d$ and $H = 10\,d$.

With reference to the weakly advected region (near field)

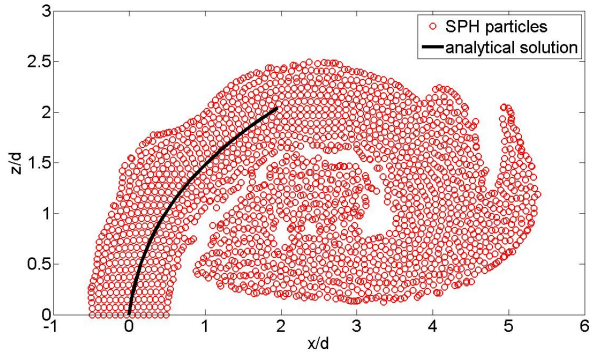

Fig. 4. SPH particle configuration of buoyant jet in crossflow compared with the analytical trajectory of the core jet for $t(U_0/d) = 10.0$, $V_1/U_0 = 2.0$ and $\rho_0/\rho_1 = 1.030$.

and the strongly advected region (far field), the horizontal component of velocity at the jet core evaluated by SPH is compared, respectively, with the following analytical solutions [18]:

$$\begin{cases} u(z < z_0; x_0) = U_0 + \dfrac{U_e}{2}\, erfc\left(\dfrac{z_1 - z}{b}\right) \\ u(z \geq z_0; x_0) = U_0 + \dfrac{U_e}{2}\, erfc\left(\dfrac{z - z_2}{b}\right) \end{cases} \tag{7}$$

$$\left\{ u(z; x_0) = U_0 + U_e\, exp\left[\frac{(z - z_0)^2}{b^2}\right] \right. \tag{8}$$

where $U_e = U_1 - U_0$, x_0 is the initial jet position along x-axis, $z_0 = 5.0\,d$ is the initial core of jet axis, $z_1 = 4.5\,d$ is the initial upper jet limit, and $z_2 = 5.5\,d$ is the initial lower jet limit along z-axis and b is the jet spread, evaluated by [18]:

$$\frac{db}{dx} = k\frac{U_e}{U_e + U_0} \tag{9}$$

being the velocity spread constant, $k = 0.125$ [19]. With reference to a time interval long enough to reach steady state conditions ($t(U_0/d) = 100.0$), Fig. 5 reports the comparison between the SPH simulations of the horizontal velocity field and the analytical solution expressed by Equation (7) in the weakly advected region for $x_0/d = 1.0$ (Fig. 5a) and $x_0/d = 2.0$ (Fig. 5b). These two spatial positions are characterized by a nearly constant shape of the jet velocity. Adopting the same previous time conditions, Fig. 6 shows the simulated values of u/U_0 in comparison with the analytical ones given by Equation (8) in the strongly advected region for $x_0/d = 5.0$ (Fig. 6a) and $x_0/d = 10.0$ (Fig. 6b) where a defined gaussian shape and a reduction of the velocity is evident. A general agreement between SPH results and analytical ones can be observed in Figs. 5 and 6. It is worth noting that the separation of two mentioned flow zones occurs, in this case, at about $x_0/d \cong 3.0 \div 4.0$.

The numerical simulation of the concentration field are compared with an analytical solution deduced from the advective diffusion equation as follows [10]:

$$\begin{cases} C(z < z_0; x_0) = \dfrac{C_1}{2}\, erfc\left(\dfrac{z_1 - z}{\sqrt{\frac{4\,D\,x_0}{U_e}}}\right) \\ C(z \geq z_0; x_0) = \dfrac{C_1}{2}\, erfc\left(\dfrac{z - z_2}{\sqrt{\frac{4\,D\,x_0}{U_e}}}\right) \end{cases} \tag{10}$$

where the diffusion coefficient, D, is set to $5 \cdot 10^2\, m^2/s$. This values proves to be in agreement with the empirical values of D adopted for applications in water streams [10].

As in the case of the horizontal velocity field, Fig. 7 highlights the comparison between SPH simulations and analytical solution given by Equation (10) in the weakly advected region for $x_0/d = 1.0$ (Fig. 7a) and in the strongly advected region for $x_0/d = 5.0$ (Fig. 7b). The concentration field highlights an exponential decay in the upper and lower zone of the axis of the jet core when the flow exceeds the zone near the jet nozzle.

Fig. 8 reports the SPH simulations referred to the time evolution of the jet, the horizontal component of velocity and the concentration field for $t(U_0/d) = 5.0$, 10.0 and 20.0. The adopted spatial resolution is $dx = 0.01d$. The spatial configurations of the jet are shown in Figs. 8a, 8d and 8g. At first an initial *horseshoe* shape of the jet occurs, followed by some vortices at the upper and lower boundary of the jet tip due to the progressive jet-water interaction. The principal jet direction moves toward the water surface. This phenomenon leads to a growth of vortical structures influencing also the water level.

Figs. 8b, 8e and 8h show the horizontal velocity field, u/U_0, for the mentioned time steps. A temporal decay in the magnitude of jet velocity induced by friction offered by the ambient flow can be observed. The concentration field, C/C_1, being C_1 the initial jet concentration, is shown in Figs. 8c, 8f and 8i. A larger vortex at the lower boundary with respect to the upper one can be noticed. This phenomenon leads to a successive general counter-clockwise rotation of the concentration field near the jet tip.

IV. Conclusion

The work is concerned with a SPH-based model for the analysis of buoyant and non-buoyant jets propagating into water streams. The algorithm proposed by Federico et al. [6] for the enforcement of upstream/downstream flow condition has been extended to model two-phase flows through a suitable set of inflow-jet particles. The model allows to simulate open-channel flows in uniform, non-uniform or unsteady regime. In addition the adopted equations of fluid mechanics have been coupled with an advective diffusion equation within the framework of the SPH formalism.

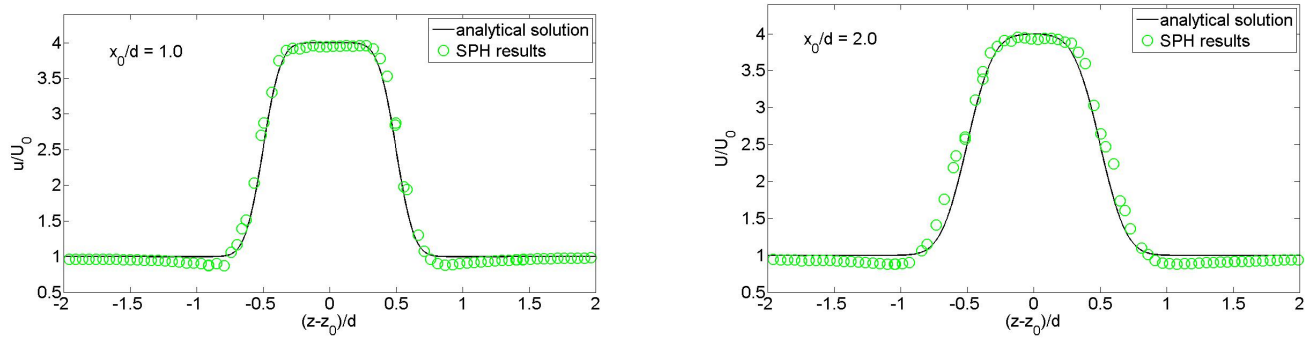

(a) (b)

Fig. 5. Non-buoyant jet in coflow: comparisons between analytical solution of horizontal velocity and numerical results at $t(U_0/d) = 100.0$ in the weakly advected region for $x_0/d = 1.0$ (a) and $x_0/d = 2.0$ (b).

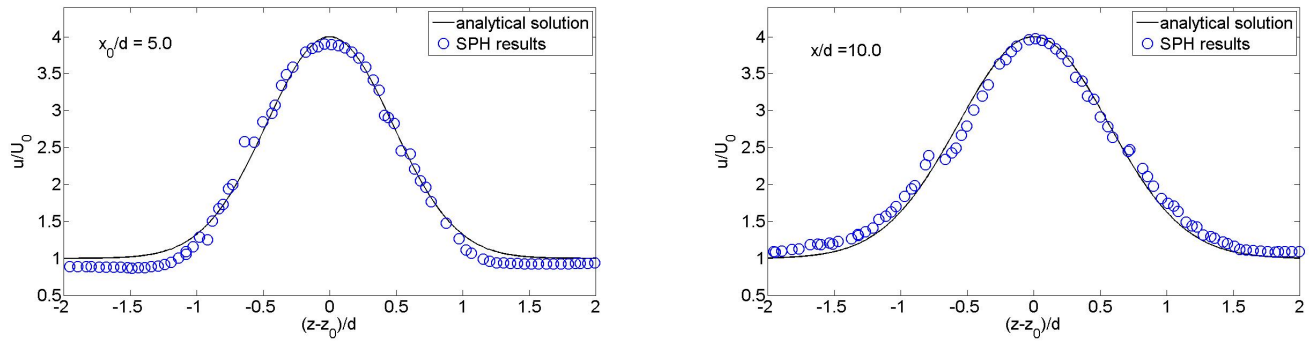

(a) (b)

Fig. 6. Non-buoyant jet in coflow: comparisons between analytical solution of horizontal velocity and numerical results at $t(U_0/d) = 100.0$ in the strongly advected region for $x_0/d = 5.0$ (a) and $x_0/d = 10.0$ (b).

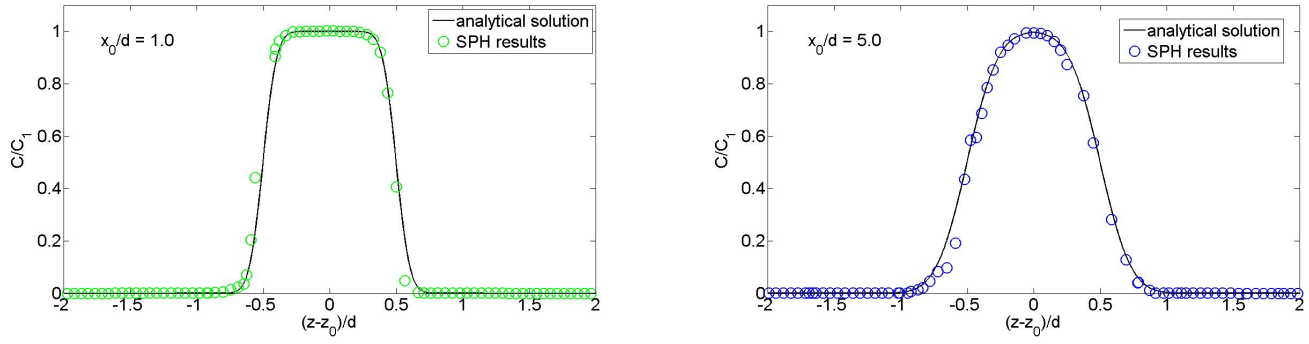

(a) (b)

Fig. 7. Non-buoyant jet in coflow: comparisons between analytical solution of concentration field and numerical results at $t(U_0/d) = 100.0$ in the weakly advected region for $x_0/d = 1.0$ (a) and in the strongly advected region for $x_0/d = 5.0$ (b).

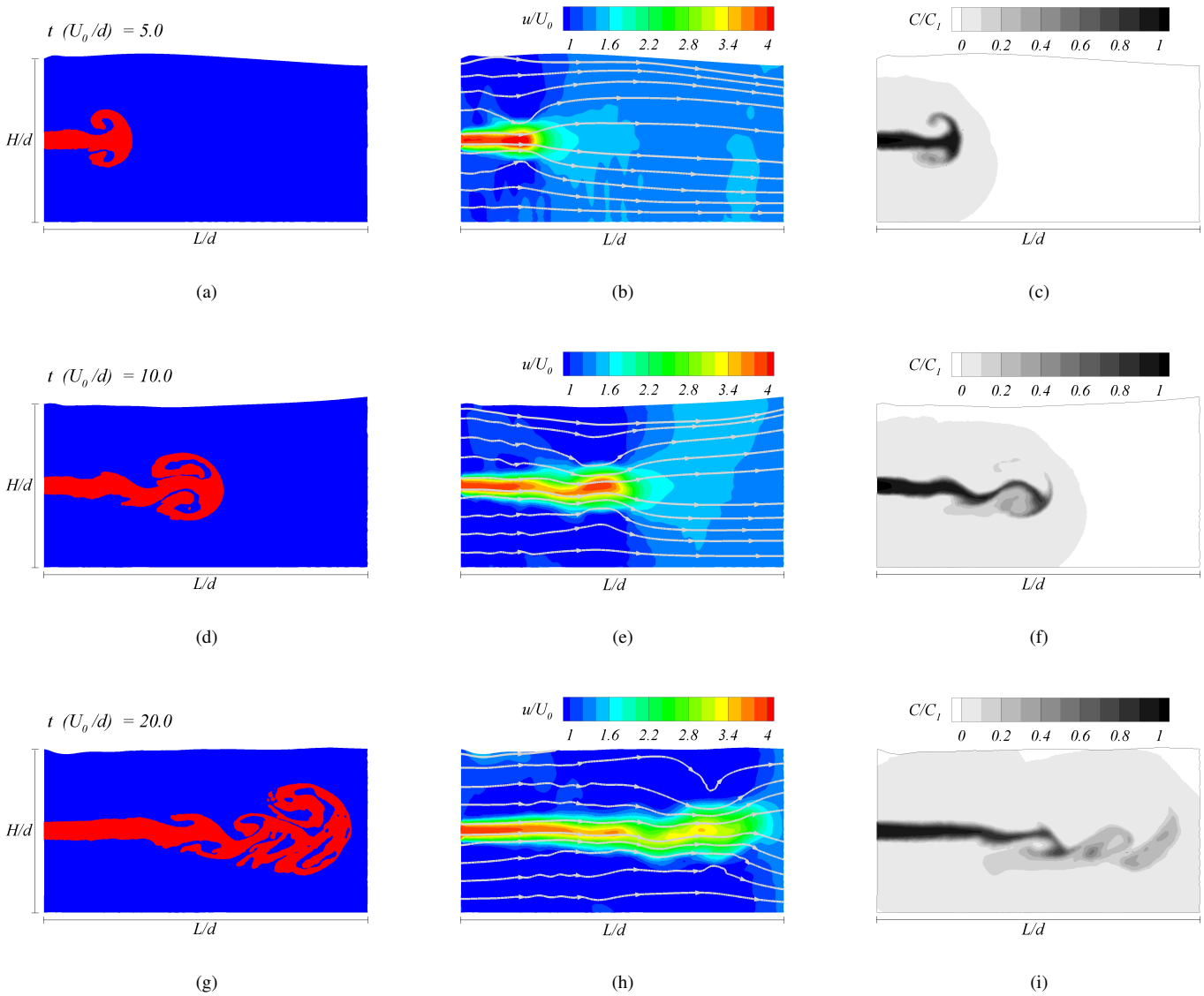

Fig. 8. Non-buoyant jet in coflow: time-evolution of the jet [(a), (d), (g)], horizontal component of velocity [(b), (e), (h)] and concentration field [(c), (f), (i)] for $t(U_0/d) = 5.0$, 10.0 and 20.0.

Continuous jets in cross-flow and co-flow in shallow water conditions are tested varying the inlet velocity and analyzing the evolution of the flow field (jet trajectories and velocities) and the associated concentration. The results obtained by SPH have been compared with analytical methods, showing an overall good agreement near the jet nozzle and far away. The proposed SPH model could be extended through appropriate boundary conditions to study counterflow and multiple jets.

ACKNOWLEDGMENT

This work has been partially supported by European Community's Seventh Framework Programme (FP7/2007-2013) under grant agreement No. 225967 "NextMuSE".

REFERENCES

[1] H.B. Fischer, E.G. List, R.C.Y. Koh, J. Imberger and N.H. Brooks. *Mixing in Inland and Coastal Waters*. Academic Press, New York, 1-483, 1979.

[2] I.R. Wood, R.G. Bell and D.L. Wilkinson. *Ocean disposal of wastewater*. Advances Series on Ocean Engineering, World Scientific, Singapore, 1-425, 1993.

[3] G.H. Jirka. *Integral Model for Turbulent Buoyant Jets in Unbounded Stratified Flows. Part I: Single Round Jet*. Environmental Fluid Mechanics, 4, 1-56, 2004.

[4] J. Kajtar and J.J. Monaghan. *SPH simulations of swimming linked bodies*. Journal of Computational Physics, 227, 8568-8587, 2008.

[5] M. Lastiwka, M. Basa and N.J. Quinland. *Permeable and non-reflecting boundary conditions in SPH*. International Journal for Numerical Methods in Fluids, 61(7), 709-724, 2009.

[6] I. Federico, S. Marrone, A. Colagrossi, F. Aristodemo and P. Veltri. *Simulating free-surface channel flows through SPH*. Proceeding of V International Spheric SPH Workshop, Manchester, UK, 90-97, 2010.

[7] N. Grenier, M. Antuono, A. Colagrossi, D. Le Touzé and B. Alessandrini. *An Hamiltonian interface SPH formulation for multi-fluid and free surface flows*. Journal of Computational Physics, 228, 8380-8393, 2009.

[8] F. Aristodemo, I. Federico, P. Veltri and A. Panizzo. *Two-phase SPH modelling of advective diffusion processes*. Environmental Fluid Mechanics, 10, 451-470, 2010.

[9] T. Belytschko, Y. Krongauz, J. Dolbow and C. Gerlach. *On the completeness of meshfree particle methods*. International Journal for Numerical Methods in Engineering, 43, 785-819, 1998.
[10] S.A. Socolofsky and G.H. Jirka. *Special Topics in Mixing and Transport Processes in the Environment*. Texas AM University, 1-172, 2004.
[11] P.W. Cleary and J.J. Monaghan. *Conduction modelling using Smoothed Particle Hydrodynamics*. Journal of Computational Physics, 148, 227-264, 1999.
[12] S. Marrone, M. Antuono, A. Colagrossi, G. Colicchio, D. Le Touzé and G. Graziani. *δ-SPH model for simulating violent impact flows*. Computer Methods in Applied Mechanics and Engineering, 200, 1526-1542, 2011.
[13] T.P. Fries and H.G. Matthies. *Classification and Overview of Meshfree Methods*. Informatikbericht 2003-3, Technical University Braunschweig, 1-122, 2004.
[14] G.A. Kikkert. *Buoyant jets with two and three-dimensional trajectories*. PhD Thesis, University of Canterbury, 1-327, 2006.
[15] C.T. Crowe and H. Riesebieter. *An analytical and experimental study of jet deflection in a crossflow*. Fluid Dynamics of Rotor and Fan Supported Aircraft at Subsonic Speeds, AGARD Preprints, 1967.
[16] G.R. Jones, J.D. Nash, R.L. Doneker and G.H. Jirka. *Buoyant surface discharges into water bodies. I: flow classification and prediction methodology*. Journal of Hydraulic Engineering, 133(9), 1010-1020, 2007.
[17] P.N. Papanicolaou, J.N.E. Papaspyros, E.G. Kastrinakis and S.G. Nychas. *A heated vertical buoyant jet in a cross flow*. Mixing and dispersion in stably stratified flows, Oxford University Press, 355-373, 1999.
[18] H.J. Wang. *Jet interaction in a still or co-flowing environment*. PhD Thesis, Hong Kong University, 1-360, 2000.
[19] R.P. Patel. *Turbulent jets and wall jets in uniform streaming flow*. The Aeronautical Quarterly, 22, 311-326, 1971.